Calculation of Electrostatic Effects at the Amino Terminus of an α Helix

Doree Sitkoff,*‡ David J. Lockhart,§ Kim A. Sharp,‡ and Barry Honig*

Department of Biochemistry and Molecular Biophysics,* Columbia University, New York, New York 10032; Department of Biochemistry and Biophysics,‡ University of Pennsylvania, Philadelphia, Pennsylvania 19104; Whitehead Institute for Biomedical Research, Department of Biology,§ Massachusetts Institute of Technology, Cambridge, Massachusetts 02142 USA

ABSTRACT It is generally believed that the electrostatic field arising from the dipolar charge distribution in α helices is important for protein structure and function. We report a calculation of the electrostatic potential and field at the amino terminus of an α helix in water, obtained from a finite difference solution to the Poisson-Boltzmann equation. This method takes into account the detailed helix shape and charge distribution, as well as solvent, and generalized ionic strength effects. The calculated potential and field are found to be in good agreement with the experimentally observed helix-induced Stark effect and pK_a shifts of a probe at the N-terminus of a stable, monomeric α-helical peptide (Lockhart and Kim, 1992, 1993). Ionic screening effects are reproduced at low salt concentrations. Deviations at higher salt concentrations may result from specific ion effects (specific ion-solute and/or ion-solvent interactions). The FDPB method was used to analyze the contributions from each residue, charged side chains, and solvent to the helix potential and field. Backbone contributions come primarily from the first one to two helical turns. Charged side chains contribute to helix-induced pK_a shifts for certain probe-peptide combinations, even at relatively large distances from the probe (>14 Å).

INTRODUCTION

The charge distribution in a helix peptide backbone is believed to play an important role in protein folding, protein stability, ligand binding, enzymatic reactions, and charge transfer processes. Electrostatic interactions with helix peptide dipoles have been the subject of a number of experimental and theoretical studies in recent years (Hol, 1985; Shoemaker et al., 1987; Daggett et al., 1989; Goodman and Kim, 1989; Aqvist et al., 1991; Nicholson et al., 1991; Tidor and Karplus, 1991; Sancho et al., 1992; Lodi and Knowles, 1993). The complexity of the systems, however (which include the protein itself, the surrounding solvent and salt ions), and the large number of compensating effects that may be present such as protein relaxation or changes in both the folded and unfolded state stability, complicate the interpretation of both experimental and theoretical results.

Recently, electrostatic effects at helix termini were studied experimentally by Lockhart and Kim (1992, 1993) using a simple model system consisting of a probe molecule covalently attached to the N-terminus of peptides in either helical or random coil conformations. The interactions of the helix backbone dipoles with charges and dipoles located at the helix terminus were determined through measurement of the pK_a and Stark effect shifts of the probe molecule. The exceptional stability of the helical peptides and the overall simplicity of the experimental system allowed the results to be interpreted directly in terms of the relative strengths of solvent screening for dipole-dipole and charge-dipole interactions.

In this paper, we use continuum electrostatics to study the helix-induced pK_a and Stark effect shifts of the bound probe molecules. The approach relies on finite difference solutions to the Poisson-Boltzmann equation for polarizable solutes of arbitrary shape embedded in a dielectric medium (FDPB method) (Sharp and Honig, 1990). The FDPB method has recently been shown to yield pK_a shifts in good agreement with experimental values for ionizable residues in proteins (Bashford and Karplus, 1990; Beroza et al., 1991; Bashford and Gerwert, 1992; Gilson, 1993; Yang et al., 1993). Finite difference, boundary element, and finite element (PB) methods have also been used to calculate the effects of solvent on the absorption or fluorescence properties of chromophores. Such studies have primarily involved isolated small molecules in a uniform solvent (Bonaccorsi et al., 1983; Luzhkov and Warshel, 1991; Fox et al., 1993), although recently the ionic strength effects on the fluorescence properties of the heme in cytochrome *c* were qualitatively reproduced using the FDPB approach (Anni et al., 1994). In the work presented here we use the FDPB method to quantitatively compute the shifts in pK_a and in the absorption and fluorescence maxima of probe molecules due to the combined effects of the attached peptide and solvent. Excellent agreement with the experimentally measured shifts is obtained. We additionally use the method to provide a detailed account of the structural origins of helix-induced effects on the covalently bound probes.

The results obtained in this study demonstrate that the primary contributions from the helix peptide backbone result from the first and second helical turns. Charge-charge contributions in both the folded and unfolded states are examined, and are found to be significant at large

Received for publication 8 July 1994 and in final form 27 September 1994.

Address reprint requests to Department of Biochemistry and Molecular Biophysics, Columbia University, 630 W. 168th St., New York, NY 10032. Tel.: 212-305-7970; Fax: 212-305-6926; E-mail: Honig@cuhhca.hhmi.columbia.edu.

David J. Lockhart's current address is Affymetrix, 3380 Central Expressway, Santa Clara, CA 95051.

0006-3495/94/12/2251/10 $2.00

distances (>14 Å). The effect of salt on the shifts is reproduced up to physiological ionic strengths. The combined experimental and theoretical approaches provide detailed information regarding the nature and relative strengths of interactions occurring at a site near the boundary between a structured peptide and the solvent. The simplicity of the system makes it an ideal model for studying factors that influence electrostatic interactions in proteins.

THEORY AND METHODS

Experimental system

Much of the experimental work has been described previously in detail (Lockhart and Kim, 1992, 1993). This section consists of a brief review with new experimental work appearing at the end of the section.

Experiments were performed on the 21-residue model peptides shown below. The probe groups 4-methylaminobenzoyl (MABA), 4-carboxybenzoyl terephthalate (TPA), and succinylic acid (SUC), shown in Fig. 1, were covalently linked through an amide bond to the N-terminus of the peptides.

F_s —AAAAA(AAARA)$_3$A—$CONH_2$

U_s —AAPAA(APARA)$_3$A—$CONH_2$

F_sR5 —(AAAAR)$_4$A—$CONH_2$

U_sR5 —(AAPAR)$_4$A—$CONH_2$

The helical (F) peptides consist primarily of alanine. The random coil (U) peptides are nearly identical in composition to the F peptides but contain several proline residues to disrupt helix formation. All peptides contain several arginines to ensure solubility in water. Structural examination of the peptides using circular dichroism (CD) spectroscopy and two-dimensional nuclear magnetic resonance (NMR) experiments show the F peptides to be >90% helical at 0°C, with little fraying at the amino termini. The nuclear Overhauser effect data are consistent with α-helical, not 3_{10}-helical, structure. The random coil peptides are monomeric and unstructured, as determined by CD measurements.

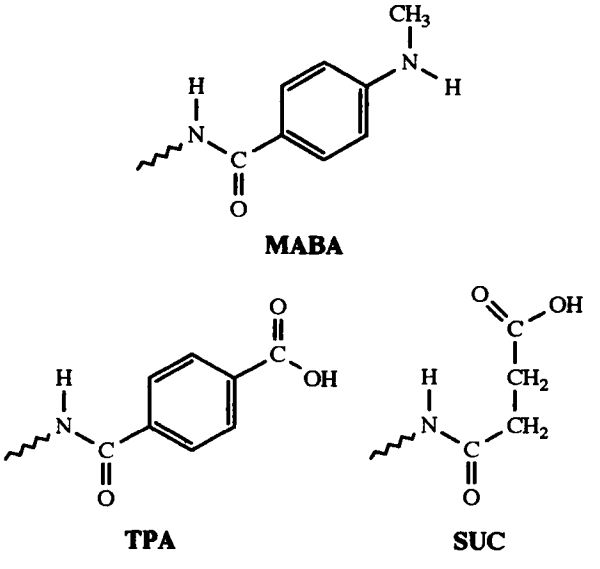

FIGURE 1 Structures of the neutral forms of the probe groups MABA, TPA, and SUC, including the amide link to the N-terminus of the peptide.

The effect of the helix backbone at the site of the probe molecules was investigated through measurement of shifts in the probe's absorption maximum and pK_a for the U versus F peptides. For MABA, the absorption band centered near 295 nm was monitored (maximum extinction coefficient of ~19000 $M^{-1}\cdot cm^{-1}$). Shifts in absorption maxima for MABA were measured at 0°C and pH 7. pK_as of the MABA and TPA probes were determined from the pH dependence of the absorption bands centered near 295 nm for MABA and 243 nm for TPA. The pK_a of SUC was determined by monitoring by NMR the ^{13}C chemical shift of the specifically labeled SUC carboxyl carbon at 3°C. Covalently attached MABA, TPA, and SUC all titrate with pK_as in the range of pH 3–pH 5.

All experiments were done in a buffer containing 1 mM sodium citrate, 1 mM sodium phosphate, and 1 mM sodium borate. Ionic strength effects were tested by increasing the concentration of NaCl from 0 to 4 M.

In new work, shifts in the fluorescence maximum of MABA were measured. Data were collected at 0°C and pH 7. To investigate possible specific ion effects, ionic strength effects in the presence of $MgSO_4$ were determined.

Electrostatic theory

The Stark effect on absorption or fluorescence

In the presence of an electric field, a shift is induced in the absorption or fluorescence maximum of the probe group, corresponding to a change in electronic transition energy. The shift can be understood by considering the probe ground and excited electronic states as dipoles interacting with the electric field. The energy of a dipole $\boldsymbol{\mu}$ in an electric field $\mathbf{E}$ is given by $-\boldsymbol{\mu}\cdot\mathbf{E}$. Thus, the energy levels of a molecule in a field are each shifted by the amount $-\boldsymbol{\mu}_i\cdot\mathbf{E}$, where $\boldsymbol{\mu}_i$ is the dipole moment of state i (see Fig. 2). If the molecule undergoes a transition between states, the excitation energy will be shifted due to the electric field by $-\Delta\mathbf{d}\boldsymbol{\mu}\cdot\boldsymbol{E}$, where $\Delta\boldsymbol{\mu}$ is the difference in dipole moments of the electronic energy states. The interaction energy expression $-\boldsymbol{\mu}_i\cdot\mathbf{E}$ is exact if the field is constant over the entire molecule; otherwise it must be replaced by the summation $\sum_j q_{i,j}\phi_j$, where $q_{i,j}$ and ϕ_j are the ith state charge and potential at position j, respectively; the shift in interaction energy would then be given by $\sum_j \Delta q_j\phi_j$ where Δq_j is the change in charge and ϕ_j is the potential at position j, respectively.

In the system studied here the probe is placed in two different environments, corresponding to the covalently attached helical or random coil peptides (see Fig. 3). The net Stark effect ($\Delta h\nu$) corresponding to the difference between steps 2 and 1 of Fig. 3 is given by:

$$\begin{aligned}\Delta h\nu_{abs,fluor} &= -\Delta\boldsymbol{\mu}\cdot(\mathbf{E}^{H}-\mathbf{E}^{RC})\\ &= -\Delta\boldsymbol{\mu}\cdot(\mathbf{E}^{H}_{pep,scr}-\mathbf{E}^{RC}_{pep,scr})\\ &\quad + -\boldsymbol{\mu}_f\cdot(\mathbf{E}^{H^f}_{prrf}-\mathbf{E}^{RC^f}_{prrf})+\boldsymbol{\mu}_i\cdot(\mathbf{E}^{H^i}_{prrf}-\mathbf{E}^{RC^i}_{prrf})\end{aligned} \quad (1)$$

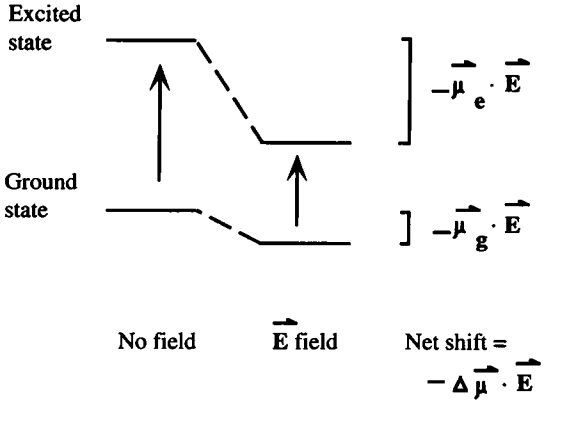

FIGURE 2 Effect of an electric field $\mathbf{E}$ on the energy difference between two states with dipole moments $\boldsymbol{\mu}_g$ and $\boldsymbol{\mu}_e$. The net change in the transition energy is given by $-\Delta\boldsymbol{\mu}\cdot\mathbf{E}$, where $\Delta\boldsymbol{\mu} = \boldsymbol{\mu}_e - \boldsymbol{\mu}_g$.

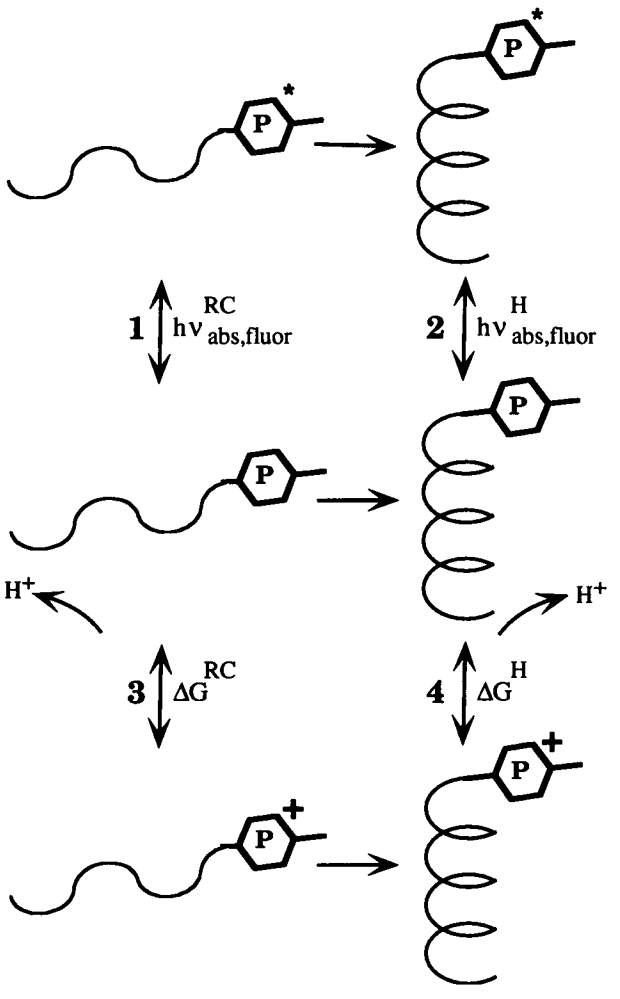

FIGURE 3 Schematic showing the processes associated with the Stark effect ($h\nu^{RC}$ and $h\nu^{H}$) and pK_a shift (ΔG^{RC} and ΔG^{H}) measurements, and their relationship to the energies conferred by the change in peptide conformation (horizontal arrows). The net helix-induced Stark and pK_a shifts are given by $h\nu^{H} - h\nu^{RC}$, and $(\Delta G^{H} - \Delta G^{RC})/2.303RT$, respectively.

where the superscripts *H* and *RC* denote the peptide in the helical or random coil conformation, *i* and *f* are the initial and final states of the probe (ground and excited for absorption, vice versa for fluorescence) and $\mathbf{E}_{pep,scr}$ is the field due to the solvent-screened peptide partial charges. The probe reaction field ($\mathbf{E}_{pr\ rf}$) results from the response of the solvent to the distribution of charge in the probe. This response may be different when the peptide is helical due to the displacement of solvent from the proximity of the probe by the helix (in the continuum electrostatic description this results from the difference in the shape of the peptide-solvent dielectric boundary).

$\mathbf{E}_{pr\ rf}$ can also change in response to differences in the charge distribution of the initial and final states of the probe. However, because the optical transition takes place on a time scale too short for solvent reorganization to occur (fs time scale), the reaction field of the probe in the final state ($\mathbf{E}^{f}_{pr\ rf}$) differs from the reaction field of the initial state ($\mathbf{E}^{i}_{pr\ rf}$) only in the high-frequency dielectric response of the solvent (electronic polarization), which is small in comparison with the translational and reorientational responses in polar solvents. Thus, in the absorption Stark shift experiments, both ground and excited state probe dipole moments interact primarily with reaction field of the ground state dipole moment. Likewise in fluorescence, the dipole moments interact primarily with the reaction field of the excited state probe, because the solvent can equilibrate during the excited state lifetime (ns time scale). The difference in $\mathbf{E}_{pr\ rf}$ for the ground and excited electronic states of the probe leads to an experimentally observed difference (Stokes shift) between the excitation and emission energies of the probe. In the peptide system studied here, the presence of the attached peptide alters $\mathbf{E}_{pr\ rf}$ in the ground and excited states, producing a change in the Stokes shift, as will be described in further detail below.

pK_a shifts

pK_as are shifted due to electrostatic interactions between the titrating group and the environment in a manner analogous to the Stark effect shift described by Eq. 1. In the pK_a case, the shift may be calculated by summing the changes in energy given by $q\phi$, or charge multiplied by potential, at all sites in the system (Gilson and Honig, 1988; Loewenthal et al., 1993). The time scale of the protonation process is long enough that both the high- and low-frequency dielectric responses of the solvent contribute. Therefore, both the neutral and ionized state charges interact with their respective fully equilibrated solvent reaction potentials. The calculated pK_a shift is thus given by:

$$\Delta pK_a = \frac{\Delta q(\phi^{H}_{pep,scr} - \phi^{RC}_{pep,scr}) + q^{\circ}(\phi^{^{\circ}H}_{pr\ rf} - \phi^{^{\circ}RC}_{pr\ rf}) - q^{+}(\phi^{^{+}H}_{pr\ rf} - \phi^{^{+}RC}_{pr\ rf})}{2.303RT} \quad (2)$$

where q and ϕ are the charge and potential at the protonation site, Δq is the change in charge upon deprotonation, and the superscripts $^{\circ}$ and $^{+}$ indicate the deprotonated and protonated probe states, respectively (other abbreviations are as in Eq. 1).

Electrostatics calculations

Electrostatic potentials and fields for the peptide-linked probe molecules in solvent were calculated using the DelPhi program (Gilson et al., 1987; Nicholls and Honig, 1991), which yields numerical solutions to the PB equation

$$\nabla\epsilon(\mathbf{r})\nabla\phi(\mathbf{r}) - \epsilon\kappa^2\sinh[\phi(\mathbf{r})] + 4\pi\rho(\mathbf{r})/kT = 0. \quad (3)$$

The solute is represented explicitly by a set of atomic coordinates with associated atomic radii and partial charges. Solute polarizability is included through the solute (internal) dielectric constant. The boundary between solute and solvent is defined by rolling a solvent-sized probe (1.4 Å for water) over the solute surface, producing the "molecular surface." Solvent is represented by a dielectric continuum of the appropriate dielectric constant (e.g., 80 for room-temperature water, 88 at 0°C). Salt effects are incorporated through the Debye-Huckel parameter κ, given by $(8\pi e^2 N_A I/1000kT)^{1/2}$, where I is the ionic strength of the solution, N_A is Avogadro's number, k is Boltzmann's constant, and T is the temperature in Kelvin. The calculations include a Stern layer (electrolyte exclusion zone) of 2 Å. The solute, solvent and ions, with associated charges and dielectric and ionic boundaries, are mapped onto a grid. The PB equation is then solved using a finite difference method (Nicholls and Honig, 1991). The solution yields the electrostatic potential at every grid point. The electrostatic field is obtained as the gradient of the potential with distance. In these calculations, the linearized form of the PB equation in which $\sinh[\phi(\mathbf{r})]$ is replaced by $\phi(r)$ was used. The inclusion of higher-order terms in the expansion of $\sinh[\phi(\mathbf{r})]$ did not significantly affect the results.

The probe-peptide structures used in the electrostatics calculations were obtained through model building using the Insight/Discover program (Biosym Technologies, Inc., San Diego, CA). The (ϕ, ψ) angles (−67°,−47°) and (−120°, 120°) were used for the helical and random coil conformations (these are the default values for α helix and extended β sheet geometries in Insight/Discover). The torsion angle values for the random coil (−120°, 120°) were chosen over (180°, 180°) due to the deeper minimum in the Ramachandran plot at (−120°, 120°); however, the effect of this choice on the results is small (see below). Sensitivity of results to side chain conformation in the helical and random coil peptides was tested by building the arginine side chains in three alternative positions: fully extended (torsion angle values of 180°) and pointed toward the N- or C-terminus. The latter two were created by starting with extended side chain torsions, rotating the $\chi 1$ or $\chi 2$ angle, respectively, to the *gauche* value, and locally minimizing

the resultant arginine side chain atom positions using Discover. Results for the N- and C-terminal-directed arginine conformations differed by at most 0.07 kcal/mol (0.05 pH units) from extended side chain conformation values, which are reported below.

Atomic charges and radii were taken from the CHARMM (PARAM19) (Brooks et al., 1983), OPLS (Jorgensen and Tirado-Rives, 1988) and CVFF (Discover) (Hagler et al., 1979) force fields, and from the PARSE parameter set (Sitkoff et al., 1994) (where necessary, atomic radii were obtained from force field σ values using $r = 2^{-5/6}\sigma$). The PARSE parameters were developed recently for specific use with the FDPB method by optimizing to solvation energies of small molecules. Backbone charges and radii used in the calculations are shown in Table 1.

The solute was assigned an internal dielectric constant of 2 in accordance with experimentally measured values obtained for small organic molecules (Sharp et al., 1992); other dielectric values were also tested. Solvent was assigned a dielectric constant of 88, which is the experimentally measured bulk dielectric constant value of water at 0°C, at which temperature the experimental data were collected. All calculations assumed a baseline salt concentration of 0.003 M in accordance with the buffered state of the experimental system. Calculations were performed at a scale of 2.4 grids/Å. The scale was focused to 4.0 grids/Å for calculations of the electrostatic field at the center of the probe due to the reaction field of the probe charges. This fine grid is required when charges are in close proximity to the point at which the field is being evaluated. Energies differed by <0.1 kcal/mol when the grid scale was varied from 2 to 4 grids/Å, and by less than 0.2 kcal/mol when grid centering was varied. A constant grid center was used for all of the calculations.

Stark effect

$\Delta\mu$ in Eq. 1 (the change in dipole moment between the ground and excited states) for MABA was represented as an 8 Debye point dipole located at the center of the aromatic ring and pointing along the para-substituted axis in the direction of the methylamino ring substituent (Lockhart and Kim, 1992). The electrostatic field was calculated in the center of the ring. An alternative method was also used, in which the net $\Delta\mu$ was represented by adding partial charges to each atom such that the net change in dipole moment totaled 8 D (and the terms $-\Delta\boldsymbol{\mu}\cdot\mathbf{E}$ in Eq. 1 were replaced by $\sum_i \Delta q_i \phi_i$ where Δq_i are the added atomic partial charges). There are multiple partial charge sets that will produce the required $\Delta\mu$ magnitude and direction. Two sets that were tested are: 1) partial charges of −0.45, −0.15, and −0.15 (−*e* units) added to the carboxyl-substituted ring carbon and its two bonded ring carbons, respectively, and partial charges of 0.45, 0.15, and 0.15 added to the methylamino-substituted ring carbon and its two bonded ring carbons, respectively; and 2) partial charges of −0.14 each added to the carboxyl-substituted ring carbon and its two bonded ring carbons, partial charges of 0.14 each added to the methylamino-substituted ring carbon and its two bonded ring carbons, and partial charges of −0.15 and 0.15 added to the carboxyl carbon and amino nitrogen, respectively. Results using both charge sets agreed to within several tenths of a kcal/mol with results obtained using the 8 D point dipole representation. Detailed results are reported here for the point dipole representation. Stark effects were not calculated for probe groups other than MABA, as their $\Delta\mu$ values are less certain.

For absorption, a ground state charge distribution was required to calculate the reaction field of MABA in the ground state ($\mathbf{E}^{g}_{pr\,rf}$). Charges were obtained for each force field (CHARMM, OPLS, CVFF, and PARSE) by combining the charges for the amide, aromatic ring, and carboxyl atoms assigned by that force field. For fluorescence, it was necessary to approximate an excited state charge distribution to obtain the reaction field due to the excited probe state ($\mathbf{E}^{e}_{pr\,rf}$). This was done by adding partial charges to the atoms to produce a net change in dipole of 8 D, as described in the paragraph above. Detailed results are reported for the distribution labeled 1 above. Results using other distributions differed by several tenths of a kcal/mol but followed the same qualitative trends (see below).

pK_a shift

Changes in atomic charges upon ionization (Δq in Eq. 2) used in the calculation were 1.0 on the nitrogen in MABA, and −0.5 on each carboxylate oxygen in TPA. Results in which the proton charge was distributed over more atoms differed only by several hundredths of a kcal/mol, due to the relatively large distance between the peptide terminus and the ionization site on the probe group; an exception was the SUC group (see below). The electrostatic potential ($\phi_{pep,\,scr}$) was calculated at the atom sites whose charges change upon protonation. To calculate the reaction field of the probe ($\phi_{pr\,rf}$), atomic charge parameters for MABA for each force field (CHARMM, OPLS, CVFF, and PARSE) were obtained by combining the charges for amide, aromatic ring, and carboxyl atoms assigned by that force field, as described above. Atomic charges for TPA and SUC were obtained similarly, by combining the charges for acid, aromatic, and carboxyl atoms, and the charges for acid and aliphatic atoms, respectively.

For the pK_a calculation on the SUC group, it was necessary to consider several SUC geometries. In contrast to MABA and TPA, whose structures are restricted by the planarity associated with partial double bonds, the SUC group can conceivably adopt different conformations relative to the peptide backbone; for example, the acidic group can either extend into the solvent, or it can twist back to hydrogen bond to the helix backbone. Additionally, the preferred conformation can change with the probe's charge state and/or the nature of the attached peptide (F or U). pK_a shift calculations were performed for two cases. In the first case, the SUC group was extended into solvent in both the charged and neutral states, when the attached peptide was F and U. The extended SUC group was modeled using torsional angles of $\chi1 = -120°$ and $\chi2 = 120°$ where $\chi1$ and $\chi2$ are the torsions about the bonds between the acid group carbon and the neighboring methylene, and the two methylene groups respectively. In the second case, the extended SUC structure was used for the neutral and charged probe states; however, the neutral SUC group attached to the F peptide was modeled using $\chi1 = -67°$ and $\chi2 = -47°$. The latter case permits a hydrogen bond to be formed between the C=O group of SUC and the backbone NH of alanine 3. For the calculations in which the probe was hydrogen bonded to the backbone, computed pK_a shifts were sensitive to the detailed charge distributions on the succinylic acid atoms, due to the specific and short-range nature of the interactions with the peptide. Thus, rather than using simple unit charges for the changes in charge upon protonation (Δq in Eq. 2), values were derived by subtracting the full force field-derived charge distribution for SUC in the protonated state from that of SUC in the deprotonated state.

TABLE 1 Backbone atomic charges (−*e* units) and radii (Å)*

	Atomic charges				Atomic radii			
Atom	CVFF	OPLS	CHARMM	PARSE	CVFF	OPLS	CHARMM	PARSE
C_aH		0.20	0.10	0.00		2.19		2.00
C_a	0.12				2.18		1.90	
H	0.10				1.37		1.47	
N	−0.50	−0.57	−0.35	−0.40	1.97	1.82	1.60	1.50
H	0.28	0.37	0.25	0.40			0.80	1.00
C	0.38	0.50	0.55	0.55	2.03	2.10	1.90	1.70
O	−0.38	−0.50	−0.55	−0.55	1.60	1.68	1.60	1.50

*Values assigned to the peptide backbone atoms for the Stark and pK_a shift calculations. C_a refers to the alpha carbon. References are as follows. CVFF, Hagler et al. (1979); OPLS, Jorgensen et al. (1988); CHARMM, Brooks et al. (1983); PARSE, Sitkoff et al. (1994).

Random coil state

The shifts due to the U peptides were calculated based on the assumption that an ensemble of random coil conformations exists in the experimental sample. Consider first the unfolded state contribution to the Stark effect shift, $-\Delta\boldsymbol{\mu}\cdot\mathbf{E}^{RC}_{pep,scr}$ (from Eq. 1). Due to the vector nature of the electric field, the ensemble produces a spread of both positive and negative shifts at the probe site, and the net contribution from the random coil is effectively averaged out to 0. The Stark shift due to the U peptides was therefore assigned a priori the value of 0 in the calculation. In contrast, the electrostatic potential, which contributes to the random coil pK_a shift ($\Delta q\phi^{RC}_{pep,scr}$ from Eq. 2), is a scalar quantity, and as there is a net charge on the peptide, cancellation will not occur. This means that assuming zero contribution of the random coil state to the pK_a shift would introduce some inaccuracy into the calculated pK_a shifts, primarily due to the neglect of the potential induced by charged arginine side chains on the peptide. We have therefore calculated the pK_a shift due to the U peptides using two methods. In the first, the zero shift approximation was used. In the second, we estimated the contributions due to the charged arginine side chains in the unfolded state by calculating the potential at the probe site due to the random coil modeled as an extended β sheet structure described above $\{(\phi,\psi) = (-120°, 120°)\}$ in which only the arginine side chains are charged. pK_a shift results are presented both with and without the addition of this random coil peptide contribution.

Calculation of shift contributions

Total helix-induced shifts were calculated and compared with experimental quantities. Contributions due to each residue were obtained by calculating the shift (relative to the unfolded peptide) of a progression of partially helical structures, generated by switching the ϕ/ψ angles of the residues in the U_s peptide from β sheet to α helix values, stepwise along the peptide chain from the N- to C-terminus. Probe reaction field contributions were quantitated by calculating the shift due to the reaction field of the probe charges with the peptide in a helical versus random coil conformation. Solvent effects were computed by changing the solvent dielectric constant from 88 (water at 0°C) to 1 (vacuum). Ionic strength effects were evaluated and compared with experimental results.

RESULTS

Helix-induced shift calculations

Calculated and experimental Stark and pK_a shifts are compared in Table 2. Overall, the agreement is good over a range of probes and peptides; the error of greatest magnitude is 1 kcal/mol, however, most of the calculated shifts are within several tenths of a kcal/mol of the experimental values. The dependencies of the pK_a shift on probe identity and peptide composition are reproduced in the calculations: the shifts are larger when alanine 5 is replaced by arginine and smaller when MABA is replaced by TPA.

Variation with parameter sets

For the MABA probe attached to the F_s and U_s peptides, calculations are reported using all four parameter sets. A nearly identical Stark shift is calculated using the PARSE and CHARMM parameter sets. OPLS parameters produced a slightly smaller shift by 0.4 kcal/mol, and the CVFF set resulted in the smallest shift by 1 kcal/mol. The pK_a shifts are consistent to within 0.08 pH units using all four parameter sets. Calculations involving other probes and peptides followed the same trends with variation of parameters (i.e., underestimation of Stark shifts using CVFF, minimal dependence of pK_a shifts on parameter set). For simplicity, only results using the PARSE parameter set are reported for these systems. Unfortunately, the large number of compensating effects and their interdependency (magnitudes of partial charges on peptide and probe, screening effect of water, solute/solvent boundary) make it difficult to pinpoint sources of discrepancies in shifts calculated using different parameter sets.

Contribution of the random coil peptide

Two sets of pK_a shifts labelled 1 and 2 are reported in Table 2, corresponding to two different methods of calculating the U peptide contribution. In method 1, the unfolded peptide was assumed to contribute zero to the net shift. In method 2, the random coil contribution was estimated by calculating the potential due to the charged arginines with the peptide in the

TABLE 2 Calculated and experimental helix-induced shifts*

Peptide	Probe	crg/rad	$\Delta h\nu_{st}$		ΔpK_a		
			Calculated	Experimental	Calculated (1)	Calculated (2)‡	Experimental
$F_s - U_s$	MABA	PARSE	−1.61	−1.60	−0.51	−0.43	−0.45
		CHARMM	−1.51		−0.48	−0.41	
		OPLS	−1.26		−0.43	−0.36	
		CVFF	−0.62		−0.46	−0.38	
$F_sR5 - U_sR5$	MABA	PARSE	−1.63	−1.67	−0.65	−0.50§	−0.49
$F_s - U_s$	TPA	PARSE			−0.43	−0.35	−0.28
$F_s - U_s$	SUC	PARSE			−0.39¶, −0.98‖	−0.31¶, −0.90‖	−0.55

*Calculations assume the random coil peptide does not induce any shift, unless otherwise specified. Experimental values were measured relative to an unfolded control. $\Delta h\nu_{st}$, calculated or experimental helix-induced Stark shift; ΔpK_a, calculated or experimental helix-induced pK_a shift. Free energies are in kcal/mol, pK_a shifts are in pH units. Stark shifts are for the absorption transition. Experimental values are from Lockhart and Kim (1992, 1993).

‡Includes a nonzero shift contribution due to Arg 9, 14 and 19 in random coil structure modeled by $(\phi, \psi) = (-120°, 120°)$ and extended side chains.

§Includes a nonzero shift contribution due to Arg 5, 10, 15, and 20 in random coil structure modeled as in the preceding footnote.

¶Assumes values of −120° and 120° for torsional angles χ1 and χ2, defined as the angles about the bonds between the acid group carbon and the first methylene, and the first and second methylene groups of the SUC probe, respectively, in both neutral and charged forms, attached to the F_s and U_s peptides.

‖Assumes values of −67° and −47° for torsional angles χ1 and χ2 for the neutral SUC probe attached to the F_s peptide; otherwise conformation is as in the preceding footnote.

extended β sheet conformation as described above. Overall, the latter has the effect of reducing the shift magnitude, due to the partial cancellation of the effect of the arginines in the helix by their effect in the random coil state. For MABA attached to the F_s and U_s probes, the pK_a shifts calculated by both methods reproduced the experimental value almost equally well (maximum errors of 0.06 and 0.09 pH units). When alanine 5 was replaced by arginine, and when MABA was replaced by TPA, however, method 2 produced significantly better agreement with the experimental pK_a shifts than did method 1. The combined contribution of arginines 5, 10, 15, and 20 to the pK_a shift in the MABA-U_sR5 system is 0.15 pH units. The combined contribution of arginines 9, 14, and 19 in the TPA-U_s system is 0.08 pH units.

SUC probe

Calculated pK_a shifts for SUC are presented in Table 2 for two structures of the probe. In the first, the carbon backbone was extended into solvent in both probe ionization states for both the F and U peptides. In the second, the neutral SUC attached to the F peptide was modeled as an extension of the peptide α helix, which permits a hydrogen bond to be formed between the C=O group of SUC and the backbone NH of alanine 3 (structures are described in detail in Theory and Methods section). The calculated pK_a shifts for the two cases were slightly too small and too large in magnitude, by ~0.2 and 0.4 pH units, respectively. This may indicate that the neutral SUC group exists in either a single intermediary conformation or in a mixture of extended and α-helical geometries when it is attached to the F peptide.

Solute dielectric constant

The Stark and pK_a shifts for the MABA probe attached to the F_s and U_s peptides were recalculated using values for the solute dielectric constant between $\epsilon = 1$ and $\epsilon = 88$. The results are shown in Table 3. Shifts using the PARSE parameter set are reported (calculations using other parameter sets showed the same qualitative trends). The pK_a shifts are relatively insensitive to the solute dielectric constant. The Stark shifts showed significantly better agreement with the experimental value when a constant of 2, a value typical of small molecules, was used. This result should be contrasted with previous FDPB calculations on whole proteins in which a dielectric constant higher than 2 ($\epsilon = 4$) was adopted (Yang et al., 1993). The latter treats, in an implicit and average way, the effect of nuclear reorganization during the process being studied (e.g., ionization or binding). The absorption/emission process, however, is on a time scale too short for nuclear reorganization to occur.

Calculated contributions to shifts

Residue contributions

The incremental shift induced by each residue in the helix was computed by calculating the shift for a progression of partially helical peptide structures generated by switching the ϕ/ψ angles in the U_s peptide to α-helical values, stepwise along the peptide chain from the N- to the C- terminus. Results for the MABA probe are depicted in Fig. 4 and Table 4. The first turn contributes 88% of the total backbone-induced Stark shift, and the first two turns contribute ~85% of the total backbone-induced pK_a shift. The results clearly demonstrate that, with regard to electrostatic interactions at the helix terminus, helix length is largely insignificant beyond the first two turns, and the magnitude of the total helix dipole moment (the macrodipole) is not an important determinant of the interaction energy. This result is in agreement with other recent calculations of electrostatic effects at helix termini (Aqvist et al., 1991; Tidor and Karplus, 1991).

Solvent screening

The screening effect of the solvent can be determined by comparing the Stark and pK_a shifts calculated for MABA in water and in vacuum (solvent dielectrics of 88 and 1, respectively). Results are displayed in Table 4. The Stark shift due to the peptide backbone is reduced by solvent screening to 15% of what its value would be in vacuum. The pK_a shift is reduced even further, to 1.4% of its vacuum strength. The results demonstrate that charge-dipole interactions near surfaces are screened much more effectively than dipole-dipole interactions, in agreement with previous work (Gilson et al., 1985; Lockhart and Kim, 1993).

Charged residues

As shown in Table 4, the charged arginine side chains of residues 9, 14, and 19 contribute very little to the Stark effect shift of MABA in both the F_s and U_s peptides. In contrast, interactions with arginines are an important contributor to the pK_a shift; the arginine side chains donate 0.22 and 0.08 pH units to the shift in the F_s and U_s peptides respectively, and the net effect represents ⅓ of the total pK_a shift. In the F_sR5 and U_sR5 peptides, the contributions of arginine 5 alone to

TABLE 3 Effect of altering solute dielectric constant*

Shift	(1, 1)	(1, 88)	(2, 88)	(4, 88)	(10, 88)	(40, 88)	(88, 88)	Experimental
Stark shift	−20.53	−2.92	−1.61	−0.95	−0.55	−0.31	−0.24	−1.60
pK_a shift	−46.55	−0.53	−0.51	−0.51	−0.50	−0.49	−0.49	−0.45

*Shifts are for the MABA probe attached to peptide F_s relative to U_s. The field and potential due to the U_s peptide were assigned to be zero. Numbers in parentheses indicate solute and solvent dielectric constants used in the FDPB calculation. Calculations were performed with PARSE charges and radii. Stark shifts are in kcal/mol; pK_a shifts are in pH units.

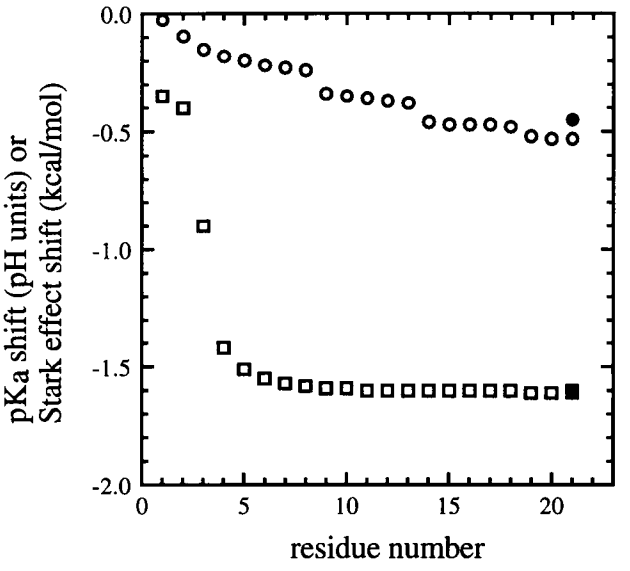

FIGURE 4 Contributions from residues to the helix-induced Stark effect and pK_a shifts. Plotted are the total shifts relative to the U_s peptide for the MABA probe attached to peptides that are helical through residue n (x axis). (○) Calculated pK_a shift. (□) Calculated Stark effect shift. (●,■) Experimental values. Increases in the pK_a shift at residues 9, 14, and 19 are due to contributions from arginine side chains.

the pK_a shifts are 0.14 and 0.08 pH units, respectively, in close agreement with the experimentally measured values (0.14 and 0.10 pH units, respectively; Lockhart and Kim, unpublished data). The results are consistent with the general rule that charge-charge interactions persist at larger distances than do charge-dipole interactions; this follows from the distance dependence of the interaction energies ($1/r$ and $1/r^2$, respectively).

A significant point is that these interactions occur over relatively large distances, particularly when compared with nonbonded cutoffs of ~10 Å frequently used in molecular dynamics methods. The breakdown of contributions and distances for each arginine residue is as follows. In the F_s peptide, arginines 9, 14, and 19 contribute 0.10, 0.08, and 0.04 pH units, respectively, at distances of ~20, 23, and 33 Å measured from the CZ atom of arginine to the nitrogen in MABA. In the U_s peptide, distances between the arginines and the MABA group are 38 Å and greater (in reality, conformational fluctuations will permit much smaller distances to occur). Arginine 5 is located at distances of 17 and 25 Å from the probe in the F_sR5 and U_sR5 peptides, respectively. The results demonstrate that electrostatic effects from charged residues >10 Å away can be significant, particularly when several such groups are present.

For the case of the unfolded state, we additionally tested the adequacy of a simple Coulomb's law interaction modified by a Debye-Huckel term to calculate the arginine contributions to pK_a shifts. To obtain the shift at probe p due to arginine i, we used the equation

$$\Delta pK_a = \frac{332(e^{-\kappa/r})q_i q_p}{2.303RT\epsilon r_{ip}} \quad (4)$$

where κ is the inverse of the Debye length (Debye length is 55.63 for an ionic strength of 0.003 M); q_i and q_p are the charges on arginine i and probe p, respectively (1.0 electron unit placed on the CZ atom in arginine and on the nitrogen atom in MABA); r_{ip} is the distance between arginine i and the probe (measured in Å between the two charged atoms); and ϵ is the dielectric constant (88 at 0°C). Eq. 4 is sufficient to reproduce the charge-charge interaction energies between the arginines and probe to within experimental error, probably due to the full exposure of the probe and side chains and extension of the peptide (this equation also provides a good estimate of charge-charge interaction energies in the helical folded state, although this is not expected to be the case for proteins in general, and particularly for interactions involving buried charges). It may therefore be easy to estimate interaction magnitudes in the unfolded state of a peptide or protein by building simple models, measuring distances between charges, and using Coulomb's law combined with simple Debye-Huckel theory.

Probe reaction field

When the peptide is in a helical conformation, solvent is displaced from the vicinity of the probe molecule. This leads to a reduction in the reaction field induced by the probe charges, and thus contributes to the helix-induced shift. The effect is to reduce the Stark shift by 0.2 kcal/mol (see Table 4). In the case of the pK_a shift, the ionization site on the MABA probe is far enough away from the peptide that the helix does not significantly disturb the solvation of the charged MABA atoms. The contribution due to the reaction field of the probe to the pK_a shift is thus effectively zero.

While the contribution of the probe reaction field to the Stark effect shift is relatively small in the case of absorption, it is expected to be larger for the fluorescence transition. The excited state of MABA is considerably more dipolar than the ground state; therefore its interaction energy with solvent is stronger. Also, recall that the instantaneous nature of the electronic transition means that both ground and excited states interact with the solvent orientation around the initially populated state, the ground state for absorption and the excited state for fluorescence. Results for the fluorescence transition are included in Table 4. To obtain the reaction field due to the probe excited state ($\mathbf{E}_{pr\ rf}$) an approximate excited state charge distribution was created from the ground state distribution by adding and subtracting charges over the ring such that the net change in dipole moment of the probe was 8 D, in the appropriate direction (see Theory and Methods for details of the charge distribution). As expected, the calculated probe reaction field contribution was much larger for the fluorescence than for the absorption transition. Interestingly, the calculated probe reaction field nearly cancels the peptide contribution to the shift (Table 4), in agreement with the experimental observation of a very small helix-induced shift in fluorescence. The difference in the contributions of the probe reaction field to the absorption and fluorescence transitions can be interpreted as a measure of the change in

TABLE 4 Contributions to Stark effect and pK_a shifts*

			Residues				Solvent			Peptide vs. probe	
	Total experimental	Total calculated	First 6 residues‡	Rest of backbone§	arginines in F_s¶	arginines in U_s¶	Backbone in vacuum‖	Backbone in water**	Fraction screened‡‡	Screened peptide§§	Probe reaction field¶¶
Stark effect (absorption)	−1.60	−1.61	−1.55	−0.04	−0.02	−0.00	−12.39	−1.80	0.85	−1.82	0.21
Stark effect (fluorescence)	~0.00	−0.38								−1.82	1.44
pK_a shift	−0.45	−0.43	−0.22	−0.07	−0.22	−0.08	−21.31	−0.30	0.99	−0.44	0.01

*Shifts are for the MABA probe attached to peptide F_s relative to U_s. The field due to the U_s peptide was assumed to be zero; the potential due to the U_s peptide was estimated using a β sheet structure (ϕ, ψ) = (−120, 120) (see Theory and Methods). Calculations were performed using PARSE charges and radii. Stark effect shifts are in kcal/mol and pK_a shifts are in pH units. Contributions to the helix-induced shifts are as follows.

‡Peptide backbone of first 6 residues including solvent screening effects and induced changes in reaction field of the probe.

§Peptide backbone of residues 7–21 including solvent screening effects.

¶Charged side chains of arginine residues 9, 14, and 19, including solvent screening effects.

‖Entire peptide backbone in the absence of solvent (solute and solvent dielectric constants of 2 and 1, respectively).

**Entire peptide backbone in water (solute and solvent dielectric constants of 2 and 88, respectively).

‡‡Fraction by which interaction energy with the peptide backbone is reduced due to presence of water.

§§Whole peptide (backbone and side chains), including solvent screening, excluding induced changes in probe reaction field.

¶¶Helix-induced changes in the probe reaction field.

the Stokes shift of the probe molecule due to the displacement of solvent by the helix.

Ionic strength effects

The helix-induced pK_a shift was strongly damped by the presence of salt, as shown in Fig. 5. At 1 M NaCl [ln(ionic strength) = 0], the pK_a shift is reduced to ~30% of the initial value. The Stark shift was damped by salt to a much lesser extent; the experimental shift at 1 M NaCl is ~80% of the initial value. The results indicate that, as with the pure solvent effect, charge-dipole interactions are more effectively screened by salt than are dipole-dipole interactions.

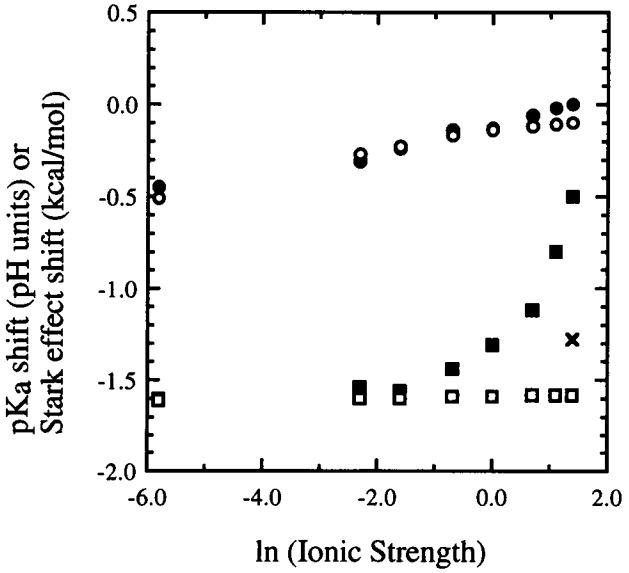

FIGURE 5 Ionic strength effects on the helix-induced Stark and pK_a shifts. (○, ●) Calculated and experimental pK_a shift. (□, ■) Calculated and experimental Stark effect shift. (x) Experimentally measured Stark effect in the presence of 1 M $MgSO_4$ (ionic strength of 4 M). All other data are for NaCl. The calculated Stark shift as a function of ionic strength is the same for both NaCl and $MgSO_4$.

The calculations reproduce most of the experimentally measured salt effects well. However, while an ionic strength effect on the Stark shift is observed, the calculated salt effect is 0. The deviations become significant above 0.2 M NaCl. The discrepancy suggests that specific salt effects, which are not considered in the FDPB method, may be present in the system. Such effects could include a general destabilization of the F helix, or specific ion interactions at the N-terminus near the probe. The measured ionic strength effect was smaller when $MgSO_4$ was used instead of NaCl, whereas the calculated results were unchanged despite the use of a larger Stern layer size. This supports the hypothesis that specific ion effects are involved; e.g., the larger size of the sulfate ions could preclude specific interactions that might be possible with the smaller chloride ions.

DISCUSSION

The α helix-spectral probe system provides a particularly well-defined system in which to study the factors that influence electrostatic fields and potentials in proteins. The use of two peptides, one of which is almost fully helical as judged by NMR and CD, the other in which the helix has been disrupted by replacing four residues with proline, allows us to examine explicitly the contribution of the α-helical conformation to the electrostatics. Also, because the helix is a small system, electrostatic interactions depend significantly on the detailed shape of the protein-solvent interface. Additionally, the use of probes that are sensitive to the field and the potential provides a more rigorous test of the electrostatics calculational methodology than studying either potentials or fields alone. The excellent agreement obtained between experimental and calculated total shifts enables us

to address, through an analysis of the contributions to the fields and potentials at the probe, the importance of these factors, as well as dielectric constants and charge-charge effects, to electrostatic interactions in proteins.

One important issue is the relevance of helix length to the strength of interactions with the helix backbone. Our calculations provide a clear demonstration that only the residues near the terminus (the first one to two turns) contribute significantly to interactions with groups at the amino terminus of an isolated peptide in water. The results from the simple peptide system studied here, in which complex effects such as tertiary interactions and protein relaxation are absent, strongly reinforce similar conclusions that were reached recently in theoretical studies on whole proteins (Gilson and Honig, 1988; Aqvist et al., 1991; Tidor and Karplus, 1991). Additionally, the simplifying concept of a helix as a macrodipole is only meaningful when considering interactions at a distance several times the length of the dipole, at which the ideal or point dipole approximation is appropriate. Since it is generally impossible to have interactions over the distance of several helix lengths within a single globular protein, we can say that the macrodipole effect, if present, is likely to have little relevance for most intraprotein interactions.

Another important conclusion that can be drawn from the results is that long-range charge-charge interactions within a peptide or protein can be important to structural stability in both the folded and the unfolded states. Frequently, molecular dynamics and free energy perturbation methods employ a cutoff of 8–10 Å in electrostatics interactions to make the simulations computationally tractable. Several studies have indicated that larger cutoffs are required to reproduce experimentally observed structures or stabilities in peptides and proteins, however (Kitson and Hagler, 1988; Loncharich and Brooks, 1989; Kitchen et al., 1990; Hamaguchi et al., 1992; Schreiber and Steinhauser, 1992). Our results show that charge-charge interactions can contribute significantly at distances even greater than 20 Å (a total of 0.22 pH units or 0.30 kcal/mol from three charged groups at distances of 20, 23, and 33 Å). Due to the highly solvated nature of the extended conformation, energetic contributions in the unfolded state from charged residues that are close in sequence can in general be easily estimated by applying Coulomb's law with a Debye-Huckel term, thereby reducing the unfolded state computational requirements.

Interactions between charges on the surface of proteins are frequently quite insensitive to the internal dielectric constant used in electrostatic calculations (Gilson and Honig, 1988). This holds for the helix-induced probe pK_a shifts (charge-dipole interactions) studied here as well. The Stark shift results (dipole-dipole interactions), however, provide an example of interactions near the solute surface that are sensitive to the internal dielectric constant. Since the absorption/emission happens on a time scale that is much faster than the helix dipole and charge reorientation, the only expected contribution to the dielectric response of the helix is electronic reorganization. Based on the experimental high-frequency dielectric constants for small organic molecules this contribution corresponds to a dielectric of ~2 (Sharp et al., 1992). It is encouraging that the best results were obtained with this value for the helix dielectric.

As our calculations show, the net field and potential at the helix N-terminus depends on the balance between the Coulombic interaction between probe and helix charges, the screening of this interaction by the solvent, and the reaction field induced in the solvent by the charges on the probe itself. In the case of protonation, the reaction field is different around the ionized and unionized probe forms. In the case of the Stark effect, however, the reaction field component due to solvent reorientation is effectively fixed because the absorption/emission happens on a much faster time scale. This leads to a different shift induced by the formation of the helix in absorption versus fluorescence. This experimental helix-induced Stokes shift is reproduced quite well in our calculations, indicating that the method treats both solvent screening and reaction field (solvation) interactions with good accuracy.

The disagreement between experiment and calculation in the one case, the Stark shift at high salt, is puzzling. However, based on the success of our other calculations, we conclude that the deviation is caused by a structural change at high salt that is not included in our calculations, i.e., either slight fraying of the helix or localization of ions at specific sites on the helix. The improved agreement obtained when a different salt was used supports this view, but further examination of this point is necessary.

In summary, we have shown that the experimental Stark and pK_a shifts can be calculated with quantitative accuracy in the solvated peptide-probe system using the FDPB method. These calculations enable us to quantitate the contributions of several important electrostatic factors including the shape and charge distribution, the relative contributions of solvent screening and solvent reaction field, and the dielectric constant of the molecule. This opens up the possibility of using this method to treat the effects of protein structure on the absorption and fluorescence of a variety of functionally interesting chromophore-containing proteins. Additionally, the results suggest applications to calculating electrostatic effects near surfaces, where much significant biochemistry occurs (e.g., enzyme-substrate association, antibody-antigen binding), but where complexity of solute-solvent boundaries frequently makes interaction energies difficult to predict.

Note added in proof—In a recent publication (Antosiewitz, J., J. A. McCammon and M. K. Gilson. 1994. *J. Mol. Biol.* 238:415–436) pK_a shifts were calculated using the FDPB method for a number of systems including the probe-peptide unit. Results from both studies are in close agreement.

We wish to thank Anthony Nicholls for continuing improvements of DelPhi and Peter Kim, in whose lab the experimental work was done. We thank An-Suei Yang, Andreas Windemuth, and Peter Kim for helpful discussions. Support from National Institutes of Health grant GM30518 (BH), National Institutes of Health Biophysical Spectroscopy Training grant GM082750 (DS), the Damon Runyon-Walter Winchell Cancer Research Fund (DJL) and the Johnson Research Foundation and NSF grant MCB92-20477 (KAS) are gratefully acknowledged.

REFERENCES

Anni, H., J. M. Vanderkooi, K. A. Sharp, T. Yonetani, S. C. Hopkins, L. Herenyi, and J. Fidy. 1994. Electric field and conformational effects of cytochrome c and solvent on cytochrome *c* peroxidase studied by high-resolution fluorescence spectroscopy. *Biochemistry*. 33:3475–3486.

Aqvist, J., H. Luecke, F. A. Quiocho, and A. Warshel. 1991. Dipoles localized at helix termini of proteins stabilize charges. *Proc. Natl. Acad. Sci. USA*. 88:2026–2030.

Bashford, D., and K. Gerwert. 1992. Electrostatic calculations of the pK_a values of ionizable groups in bacteriorhodopsin. *J. Mol. Biol.* 224: 473–486.

Bashford, D., and M. Karplus. 1990. pK_as of ionizable groups in proteins: atomic detail from a continuum electrostatic model. *Biochemistry*. 29: 10219–10225.

Beroza, P., D. R. Fredkin, M. Y. Okamura, and G. Feher. 1991. Protonation of interacting residues in a protein by a Monte Carlo method: application to lysozyme and the photosynthetic reaction center of *Rhodobacter sphaeroides*. *Proc. Natl. Acad. Sci. USA*. 88:5804–5808.

Bonaccorsi, R., R. Cimiraglia, and J. Tomasi. 1983. *Ab initio* evaluation of absorption and emission transitions for molecular solutes, including separate consideration of orientational and inductive solvent effects. *J. Comp. Chem.* 4:567–577.

Brooks, B. R., R. E. Bruccoleri, B. D. Olafson, D. J. States, S. Swaminathan, and M. Karplus. 1983. CHARMM: a program for macromolecular energy, minimization, and dynamic calculations. *J. Comp. Chem.* 4: 187–217.

Daggett, V. D., P. A. Kollman, and I. D. Kuntz. 1989. Free energy perturbation calculations of charge interactions with the helix dipole. *Chemica Scripta*. 29A:205–215.

Fox, T., N. Rosch, and R. J. Zauhar. 1993. Electrostatic solvent effects on the electronic structure of ground and excited states of molecules: applications of a cavity model based upon a finite element method. *J. Comp. Chem.* 14:253–262.

Gilson, M. K. 1993. Multiple-site titration and molecular modeling: two rapid methods for computing energies and forces for ionizable groups in proteins. *Proteins*. 15:266–282.

Gilson, M. K., and B. H. Honig. 1988. Energetics of charge-charge interactions in proteins. *Proteins*. 3:32–52.

Gilson, M. K., A. Rashin, R. Fine, and B. Honig. 1985. On the calculation of electrostatic interactions in proteins. *J. Mol. Biol.* 183:503–516.

Gilson, M., K. A. Sharp, and B. Honig. 1987. Calculating the electrostatic potential of molecules in solution: method and error assessment. *J. Comp. Chem.* 9:327–335.

Goodman, E. M., and P. S. Kim. 1989. Folding of a peptide corresponding to the α helix in bovine pancreatic trypsin inhibitor. *Biochemistry*. 28: 4343–4347.

Hagler, A. T., S. Lifson, and P. Dauber. 1979. Consistent force field studies of intermolecular forces in hydrogen bonded crystals. 2. A benchmark for the objective comparison of alternative force fields. *J. Am. Chem. Soc.* 101:5122–5130.

Hamaguchi, N., P. Charifson, T. Darden, L. Xiao, K. Padmanabhan, A. Tulinsky, R. Hiskey, and L. Pederson. 1992. Molecular dynamics simulation of bovine prothrombin fragment 1 in the presence of calcium ions. *Biochemistry*. 31:8840–8848.

Hol, W. G. J. 1985. The role of the α helix dipole in protein function and structure. *Prog. Biophys. Mol. Biol.* 45:149–195.

Jorgensen, W. L., and J. Tirado-Rives. 1988. The OPLS potential function for proteins. *J. Am. Chem. Soc.* 110:1657–1666.

Kitchen, D. B., F. Hirata, J. D. Westbrook, R. Levy, D. Kofke, and M. Yarmush. 1990. Conserving energy during molecular dynamics simulations of water, proteins, and proteins in water. *J. Comp. Chem.* 11: 1169–1180.

Kitson, D. H., and A. T. Hagler. 1988. Theoretical studies of the structure and molecular dynamics of a peptide crystal. *Biochemistry*. 27: 5246–5257.

Lockhart, D. J., and P. S. Kim. 1992. Internal stark effect measurement of the electric field at the amino terminus of an α helix. *Science*. 257: 947–951.

Lockhart, D. J., and P. S. Kim. 1993. Electrostatic screening of charge and dipole interactions with the helix backbone. *Science*. 260:198–202.

Lodi, P. J., and J. R. Knowles. 1993. Direct evidence for the exploitation of an α helix in the catalytic mechanism of triosephosphate isomerase. *Biochemistry*. 32:4338–4343.

Loewenthal, R., J. Sancho, T. Reinikainen, and A. R. Fersht. 1993. Long-range surface charge-charge interactions in proteins: comparison of experimental results with calculations from a theoretical method. *J. Mol. Biol.* 232:574–583.

Loncharich, R. J., and B. R. Brooks. 1989. The effects of truncating long-range forces on protein dynamics. *Proteins*. 6:32–49.

Luzhkov, V., and A. Warshel. 1991. Microscopic calculations of solvent effects on absorption spectra of conjugated molecules. *J. Am. Chem. Soc.* 113:4491–4499.

Nicholls, A., and B. Honig. 1991. A rapid finite difference algorithm utilizing successive over-relaxation to solve the Poisson-Boltzmann equation. *J. Comp. Chem.* 12:435–445.

Nicholson, H., D. E. Anderson, S. Dao-pin, and B. W. Matthews. 1991. Analysis of the interaction between charged side chains and the α helix dipole using designed thermostable mutants of phage T4 lysozyme. *Biochemistry*. 30:9816–9828.

Sancho, J., J. L. Neira, and A. R. Fersht. 1992. An N-terminal fragment of barnase has residual helical structure similar to that in a refolding intermediate. *J. Mol. Biol.* 224:749–758.

Schreiber, H., and O. Steinhauser. 1992. Cutoff size does strongly influence molecular dynamics results on solvated polypeptides. *Biochemistry*. 31: 5856–5860.

Sharp, K., and B. Honig. 1990. Electrostatic interactions in macromolecules: theory and applications. *Annu. Rev. Biophys. Biophys. Chem.* 19: 301–332.

Sharp, K., J. Jean-Charles, and B. Honig. 1992. A local dielectric constant model for solvation free energies which accounts for solute polarizability. *J. Phys. Chem.* 96:3822–3828.

Shoemaker, K. R., P. S. Kim, E. J. York, J. M. Stewart, and R. L. Baldwin. 1987. Tests of the helix dipole model for stabilization of α helices. *Nature*. 326:563–567.

Sitkoff, D., K. A. Sharp, and B. Honig. 1994. Accurate calculation of hydration free energies using macroscopic solvent models. *J. Phys. Chem.* 98:1978–1988.

Tidor, B., and M. Karplus. 1991. Simulation analysis of the stability mutant R96H of T4 lysozyme. *Biochemistry*. 30:3217–3228.

Yang, A.-S., M. R. Gunner, R. Sampogna, K. Sharp, and B. Honig. 1993. On the calculation of pK_as in proteins. *Proteins*. 15:252–265.